Conf-820692--2

MASTER

Consolidated Fuel Reprocessing Program

CONF-820692--2

DE82 017424

PERFORMANCE CHARACTERISTICS OF PLANE-WALL VENTURI-LIKE REVERSE FLOW DIVERTERS

G. V. Smith

Mechanical and Aerospace Engineering Department
The University of Tennessee
Knoxville, Tennessee 37916

and

R. M. Counce

Fuel Recycle Division
Oak Ridge National Laboratory*
Oak Ridge, Tennessee 37830

Submitted to the
Automatic Control Conference
Arlington, Virginia
June 14–16, 1982

*Operated by Union Carbide Corporation for the U.S. Department of Energy.

PERFORMANCE CHARACTERISTICS OF PLANE-WALL VENTURI-LIKE REVERSE FLOW DIVERTERS*

G. V. SMITH

Mechanical and Aerospace Engineering Department
The University of Tennessee
Knoxville, Tennessee 37916

R. M. COUNCE

Fuel Recycle Division
Oak Ridge National Laboratory
Oak Ridge, Tennessee 37830

The results of an analytical and experimental study of plane-wall venturi-like reverse flow diverters (RFD) are presented. In general, the flow characteristics of the RFD are reasonably well predicted by the mathematical model of the RFD, although a divergence between theory and data is observed for the output characteristics in the reverse flow mode as the output impedance is reduced. Overall, the performance of these devices indicates their usefulness in fluid control and fluid power systems, such as displacement pumping systems.

Introduction

A useful component of fluid control and fluid power systems is the reverse flow diverter (RFD). The reverse flow diverter is a generic name for a three-port device (see Fig. 1A) with a forward flow mode of fluid flowing from port 3 to port 1, whereas in the reverse flow mode, the fluid is diverted to port 2. One type of RFD is the venturi-like RFD, shown schematically in Fig. 1B, which has proven useful in displacement pumping systems[1–6]. In this device, the mechanism of diverting the reverse flow is the conversion of static to dynamic pressure in the nozzle of the RFD while the diffuser of the RFD recovers a portion of the original static pressure. The reduced static pressure at the throat of the RFD eliminates or reduces the amount of fluid flowing back to port 1. In the forward flow mode, the fluid does not flow appreciably to port 2 because of a sufficiently large output (i.e., port 2) impedance (perhaps a large hydrostatic head).

The utility of such devices in a pumping apparatus, incorporating an air piston and associated chamber, is easily envisioned. Pumping systems of this nature are reported to be used extensively in the British nuclear fuel reprocessing facilities[1–6]; a much wider application, however, is foreseen for their use in harsh chemical process environments, such as synfuel coal conversion projects[1], where ultra-reliable leak-free operation is required.

The purpose of this paper is to present a mathematical model describing the flow characteristics of a plane-wall venturi-like RFD and to compare these predictions with experimental observations.

2 Mathematical Model Development

The development of a simplified mathematical model is presented in this section for the flow characteristics of a venturi-like RFD. The flow will be assumed to be incompressible and steady (i.e., transient effects will be neglected).

2.1 Reverse flow mode

A prediction of the flow through the nozzle of the RFD is obtained from Bernoulli's equation, written between the input of the nozzle and the throat of the nozzle as

$$P_{1r} + \tfrac{1}{2}\rho V_{1r}^2 = P_t + \tfrac{1}{2}\rho V_t^2 \quad . \qquad (1)$$

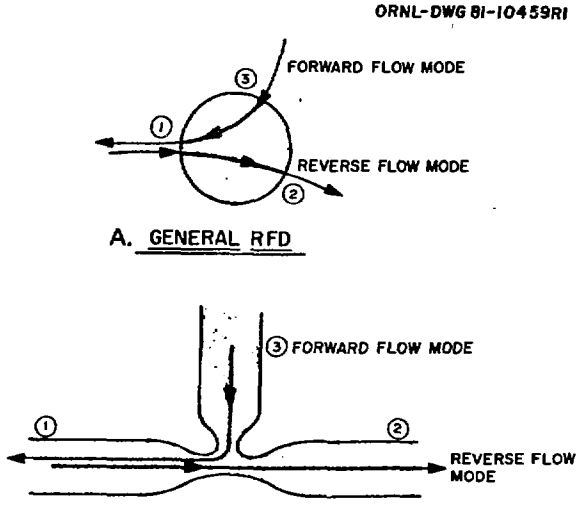

Fig. 1. Schematic of reverse flow diverter.

*Research sponsored by the Office of Nuclear Fuel Cycle, U.S. Department of Energy, under Contract No. W-7405-eng-26 with Union Carbide Corporation.

Combining the expression for the volumetric flow rate and continuity,

$$Q_{1r} = A_t V_t = A_1 V_{1r} \quad , \tag{2}$$

with Eq. (1) yields an expression for the input flow

$$Q_{1r} = C_d A_t \sqrt{\frac{2(P_{1r} - P_t)/\rho}{1 - A_t^2/A_1^2}} \quad , \tag{3}$$

where a discharge coefficient has been introduced to account for losses in the flow.

Describing the flow through the diffuser of the RFD is considerably more difficult than describing the flow through the nozzle of the RFD. The problem is very similar to the flow through the output ports of a beam deflection fluidic proportional amplifier, which has been modeled reasonably well by considering the semiconfined or planar jet impinging on the inlet to the diffuser as a "source" or "driving" pressure equal to the sum of the static and dynamic pressure of the planar jet [7]. The difference between the source (i.e., total) pressure at the diffuser inlet and the total pressure at the diffuser exit results from irreversibilities occurring in the flow between the inlet and exit of the diffuser. Mathematically, this is expressed as

$$P_s - \left(P_{2r} + \tfrac{1}{2}\rho \frac{Q_{2r}^2}{A_2^2}\right) = K_d \tfrac{1}{2}\rho \frac{Q_{2r}^2}{A_t^2} \quad , \tag{4}$$

where K_d is a diffuser loss coefficient, which is typically based on the maximum velocity occurring in the diffuser.

Perhaps a more frequently used term to represent the losses in a diffuser is the pressure-recovery coefficient, which is defined as the fraction of the inlet dynamic pressure converted to static pressure at the exit of the diffuser. The relationship between the diffuser loss coefficient and the pressure recovery coefficient is easily shown to be

$$K_d = 1 - \frac{A_t^2}{A_{2r}^2} - C_p \quad . \tag{5}$$

Substituting Eq. (5) into Eq. (4) enables it to be rewritten as

$$P_s - P_{2r} = (1 - C_p)\frac{\rho Q_{2r}^2}{2A_t^2} \quad . \tag{6}$$

It should be noted that the source pressure is equal to the total pressure at the inlet to the nozzle minus those losses which occur in the nozzle. Mathematically, this can be expressed as

$$P_s = P_{1r} - \tfrac{1}{2}\rho \frac{Q_{1r}^2}{A_t^2}\left[\frac{1 - C_d^2 - (A_t/A_1)^2}{C_d^2}\right] \quad . \tag{7}$$

Substitution of Eq. (7) into Eq. (6) results in

$$P_{1r} - P_{2r} = \frac{\rho Q_{1r}^2}{2A_t^2}\left[(1 - C_p)Q_{2r}^2\right] + \frac{\rho Q_{1r}^2}{2A_t^2}\left[\frac{1 - C_d^2 - (A_t/A_1)^2}{C_d^2}\right] \quad . \tag{8}$$

Dividing Eq. (8) by the square of Eq. (3) and manipulating algebraically enables Eq. (8) to be written in a nondimensional form as

$$\frac{P_{2r} - P_t}{P_{1r} - P_t} = C_d^2 \frac{\left[1 - (1 - C_p)(Q_{2r}/Q_{1r})^2\right]}{1 - (A_t/A_{1r})^2} \quad . \tag{9}$$

2.2 Forward flow mode

In the forward flow mode of the venturi-like RFD, as indicated by Fig. 1, the primary fluid resistance occurs at the throat of the venturi-like RFD and is nonlinear (i.e., orifice-like).

A first approximation of this flow is given by

$$Q_{3f} = C_{df} A_t \sqrt{\frac{2(P_{3f} - P_{1f})}{\rho}} \quad , \tag{10}$$

where a discharge coefficient is introduced to account for losses, and it is assumed the minimum area A_t occurs at the throat of the RFD.

3 Experimental System

The plane-wall venturi-like RFD is a laminated Plexiglas design. This design was selected because it allowed quick and economical replacement of the venturi design. The RFD is equipped with pressure sensor/transmitters to measure pressures at the entrance, throat, and discharge. Flow rates were computed from level changes in tanks associated with the fluid movement. Water at room temperature was used as the fluid being transferred in all tests. The experimental apparatus features an automatic data acquisition system by a Bristol UCS 3000 Unit Processor Controller.

A schematic of the first RFD design is shown in Fig. 2. This design used a diffuser with a double divergence angle of ~11 degrees, throat dimensions of 9.5 by 10.2 mm, and output dimensions of 9.5 by 50.8 mm; an orifice existed between port 3 and the throat of the RFD. In later studies, this resistance was reduced, as shown in Fig. 3, by adding a second inlet to the throat with a similar orifice; this modification caused the output of the nozzle to be a planar or semiconfined jet (a jet bounded on two opposite sides but free to spread in the other directions) for the length of one nozzle width to the entrance to the diffuser. In a second modification to the original design, slots (one nozzle width in

ORNL DWG. 80-7055RI

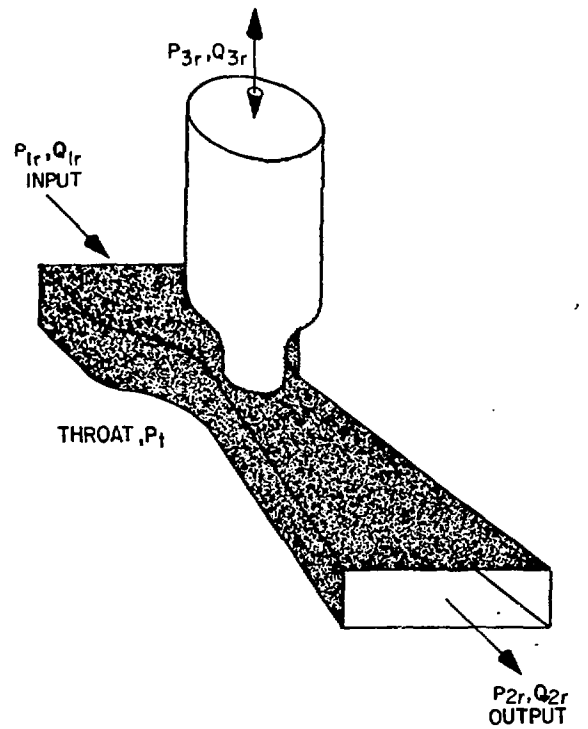

Fig. 2. Schematic of a venturi-like reverse flow diverter with a single input in the reverse flow mode.

ORNL-DWG.81-1386RI

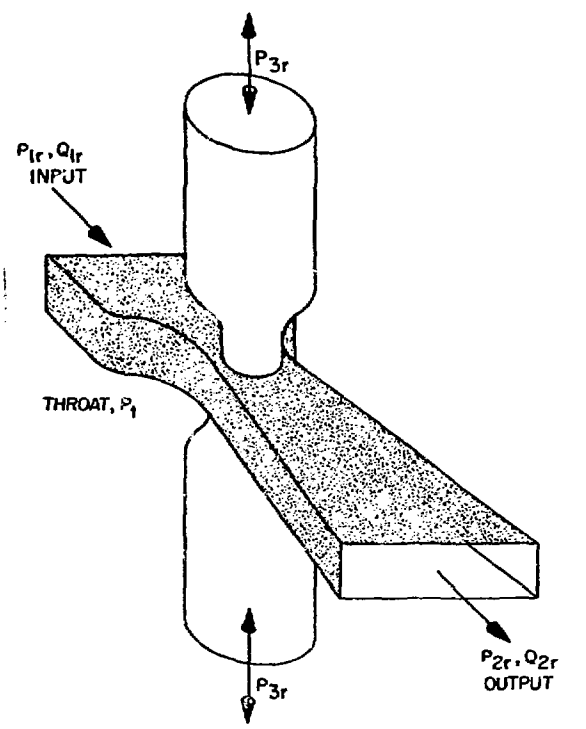

Fig. 3. Schematic of a venturi-like reverse flow diverter with a double input in the reverse flow mode.

length) were machined out of the nozzle-diffuser laminate so that the output of the nozzle was essentially a free jet.

A second RFD was constructed with throat dimensions of 12.7 by 12.7 mm, a diffuser with a double divergence angle of 6 degrees, and output dimensions of 12.7 by 37.1 mm. This design was tested with modifications one and two of the original design.

4 Results

Experimental data on the operating characteristics of the venturi-like RFD are presented in this section for both the reverse flow mode and the forward flow mode. Experimental data are compared to predictions based on the mathematical model previously discussed.

4.1 Reverse flow

The operating characteristics of the nozzle of the venturi-like RFD are presented in Fig. 4 in the form of the input flow rate vs the difference between the input pressure and the throat pressure for a discharge coefficient of 0.95. As indicated by this figure, Eq. (3) yields a good approximation to the flow through the nozzle of the RFD, as might be expected.

The output characteristics for the smaller throat RFD in the form of the output flow rate vs the output pressure are shown in Fig. 5, and the characteristics for the larger throat RFD are shown in Fig. 6. Theoretical predictions

ORNL-DWG.81-10453RI

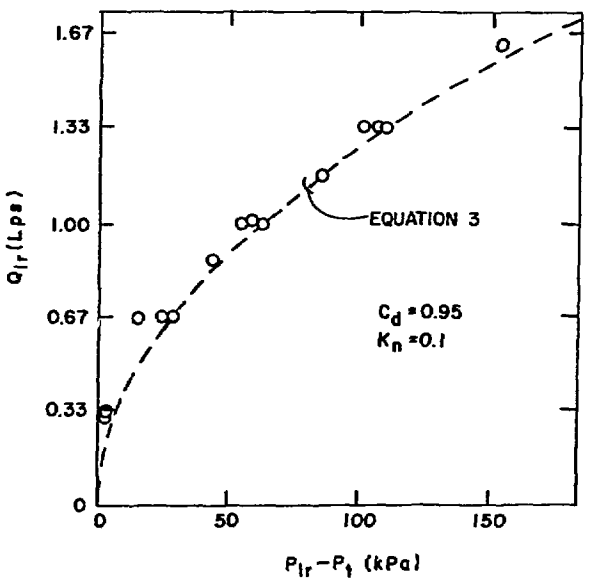

Fig. 4. Input (nozzle) characteristics in the reverse flow mode.

from the mathematical model are also shown in these figures. Generally, it is noted that the data agree with theory reasonably well at higher output pressures, although a divergence between theory and data becomes

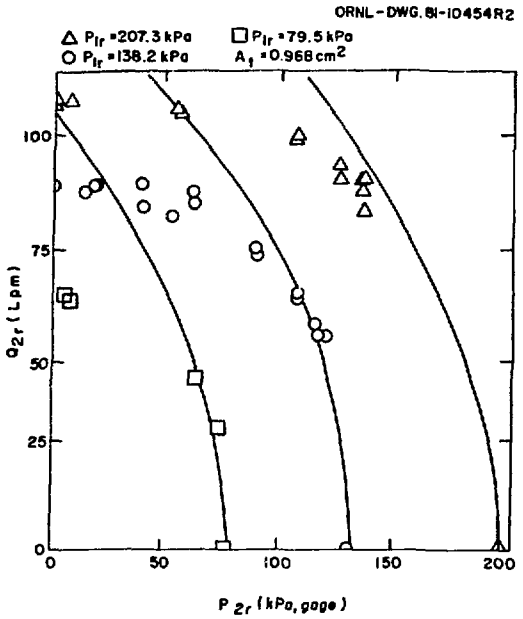

Fig. 5. Output characteristics of the smaller throat venturi-like reverse flow diverter.

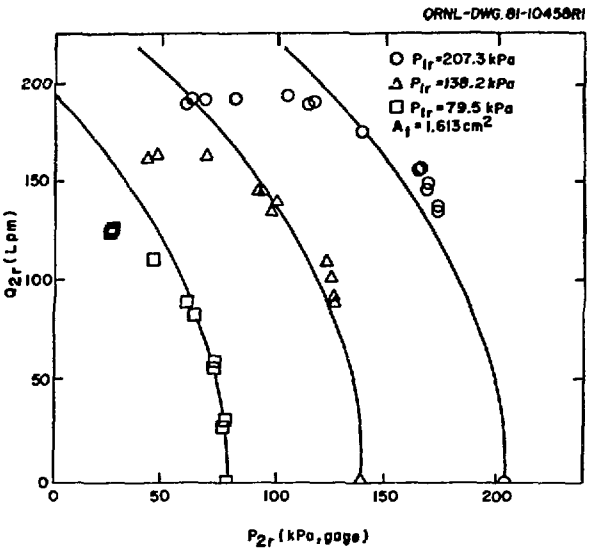

Fig. 6. Output characteristics of the larger throat venturi-like reverse flow diverter.

apparent as the output impedance is reduced. The disagreement between theory and data appears to become more pronounced as the pumping pressure is increased for both RFD's.

In an attempt to determine the cause of the disagreement between theory and experimental data at lower values of output pressure, the pressure recovery coefficient was calculated from experimental data for the first RFD tested. A portion of this information, the pressure recovery coefficient vs the output pressure, is plotted in Fig. 7. In this figure, the pressure recovery coefficient is not constant but varies significantly with the output pressure. It appears that for this smaller throat RFD, the output flow is experiencing separation for low output pressures. The negative value of the pressure recovery coefficient results in an output pressure less than the throat pressure, which indicates fully developed stall in the diffuser.

The mathematical model assumed a constant value of 0.60 for the pressure recovery coefficient for the smaller throat RFD. This value was obtained from published diffuser data[8]. Furthermore, the work of Fox and Kline[9] indicates that this diffuser design should operate in the transitory stall regime of their stability map where the maximum values of the pressure recovery coefficient are obtained. Although it is obvious that their work is based on diffusers with completely different inlet conditions, Fox and Kline have indicated that fully developed stall would not occur for this diffuser. It has been reported[8] that diffuser performance is strongly dependent on the inlet conditions.

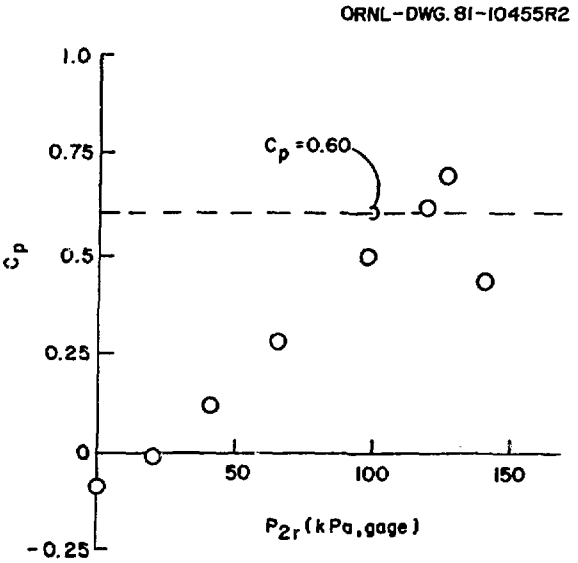

Fig. 7. Pressure recovery coefficient of the smaller throat reverse flow diverter.

Information obtained on the first RFD tested led to the design of the second (larger throat) RFD. This larger throat RFD used a smaller divergence angle in the diffuser so that it should operate in the fully stable regime of Fox and Kline's stability map[8].

The pressure recovery coefficient for the larger throat RFD plotted vs the ratio of the output pressure to the input pressure is shown in Fig. 8. It is noted that the

pressure recovery coefficient is still a strong function of the output pressure although the minimum value is still considerably larger than the minimum value achieved in the smaller throat RFD. This minimum value of pressure recovery coefficient corresponds to the output valves of the diffuser being fully opened. It is therefore evident that the larger throat RFD does not experience fully developed stall, although it still experiences a severe reduction in the pressure recovery coefficient. It is also noted that the data (Fig. 8) for various input pressures essentially collapse into a single curve. The reason for this large variation in pressure recovery coefficient with normalized output pressure is not apparent at this time.

Determining the variation of the output flow rate as a function of the input pressure while the output hydrostatic head is held constant is also of interest. Figure 9 presents this data for the larger throat RFD. For input pressures less than the hydrostatic head, the output flow rate is obviously zero; whereas for input pressures greater than the output hydrostatic head, the output flow rate increases approximately proportional to the square root of the difference between the input and output pressures, as might be expected from Eq. (6). It should be noted that the output pressure is not constant in the data presented in this figure but varies moderately because of the nonlinear viscous losses of the discharge line of the RFD output.

Equation (9) indicates that if the output pressure difference ratio, $(P_{2r} - P_t)/(P_{1r} - P_t)$, is plotted vs the normalized output flow rate, Q_{2r}/Q_{1r}, the data for different input pressures should collapse into a single curve for a given RFD. However, as will be discussed more fully in the next section, considerable effort was devoted to reducing the fluid impedance between port 3 and the throat. It was determined experimentally that this reduction resulted in the pressure at port 3 being essentially equal to the throat pressure except for the single operating condition of fully blocked load (i.e., zero output flow rate). Thus, the data are presented in the more useful format of $(P_{2r} - P_{3r})/(P_{1r} - P_{3r})$ vs Q_{2r}/Q_{1r} in Fig. 10. Also, presented in this figure are the theoretical predictions from Eq. (9). The data in this figure indicate that these nondimensional parameters tend to collapse the data into a single curve. Acceptable agreement between theory and data is observed although a divergence is still noted to exist between data and theory at lower values of output impedance.

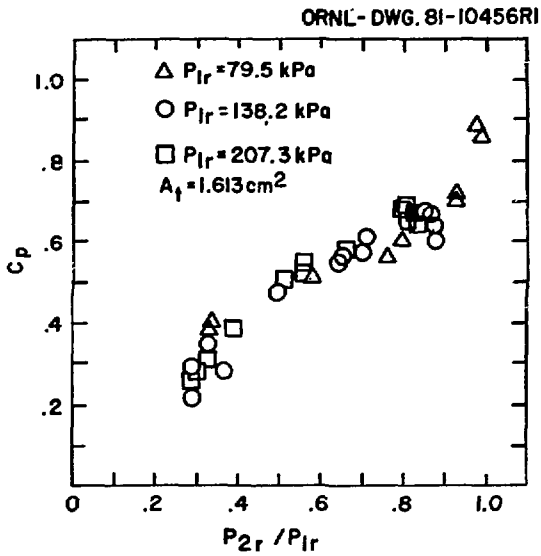

Fig. 8. Pressure recovery coefficient for the larger throat reverse flow diverter.

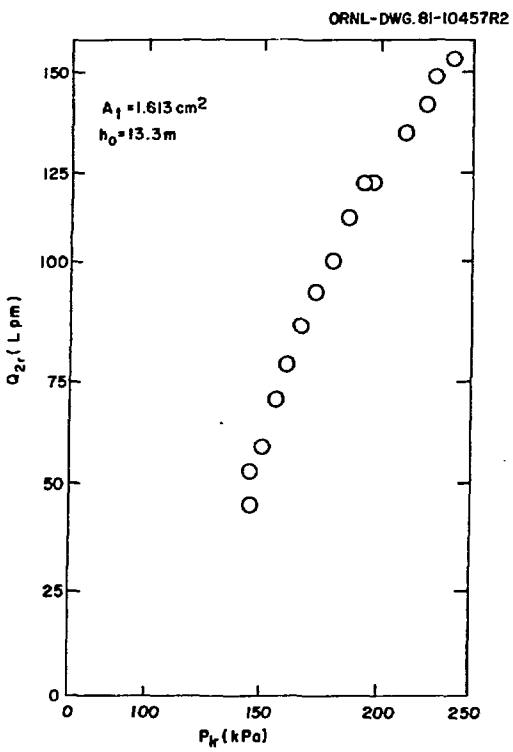

Fig. 9. Output flow as a function of input pressure; the output hydrostatic head is 13.3 m.

4.2 Forward flow mode

Since the forward flow mode is also of importance, tests were conducted with the original (smaller throat) RFD for the purpose of determining ways to reduce the fluid impedance within the RFD. Three versions of this original RFD were studied: (1) the original design with a single input to the throat from the feed tank, (2) an additional input from the feed tank added to the opposite side of the RFD, and (3) slots, one nozzle width in length and one nozzle width in depth, machined out of the laminate on each side of the throat of the RFD. In the reverse flow mode, version (2) results in the flow leaving the nozzle throat approximating a semi-confined jet before entering the diffuser of the RFD, and version (3) results in the flow emanating from the nozzle approximating a free jet before impinging on the diffuser inlet.

Table 1. Forward flow characteristics of the RFD designs

Throat condition	Forward flow rate (Lpm)	
	A_t = 0.97 cm^2	A_t = 1.61 cm^2
Single input	~23.5	
Dual input	~28.7	~58.7
Dual input with slots	~34.8	~65.5

It was expected that each alteration to the RFD should reduce the fluid impedance at the RFD throat during forward flow. Data showing the quantitative effects of these alterations on both RFD's tested are shown in Table 1.

As is evident from the data in this table, significant increases in the forward flow rate were obtained by the previously mentioned modifications to the throat of the RFD. Adding another input to the throat increased the flow rate by about 20% for the small throat RFD, whereas the addition of the slots increased the forward flow rate by almost 50% over the original design. A similar increase in forward flow rate is observed for the larger throat RFD.

It is important to note that essentially no change in the output characteristics of the RFD were observed in the reverse flow mode as a result of these modifications to the throat of the RFD.

5 Conclusions

The performance characteristics of plane-wall venturi-like RFD's presented in this study demonstrate their usefulness in fluid power systems such as displacement pumping systems. The mathematical model of the RFD predicted the operating characteristics of the RFD reasonably well although a divergence between theory and data was noted in the reverse flow mode as the output impedance was reduced.

The divergence between theory and data at low values of output impedance could be attributed to the fact that the pressure recovery coefficient of the diffuser is not constant. However, this inference is only as valid as the mathematical model of the RFD. It is probably not justified to attribute the divergence between theory and data as the cause of the variation of a single parameter in the model. Earlier work by Reid [10] has shown that the interaction between a fluid jet and a receiver is a complex phenomenon; therefore a mathematical model as simple as that presented in this study should not be expected to accurately predict data over all operating conditions. It is believed, however, that the presented model does an adequate job in predicting the operating characteristics of the RFD in the reverse flow mode when consideration is made of the simplicity of the mathematical model.

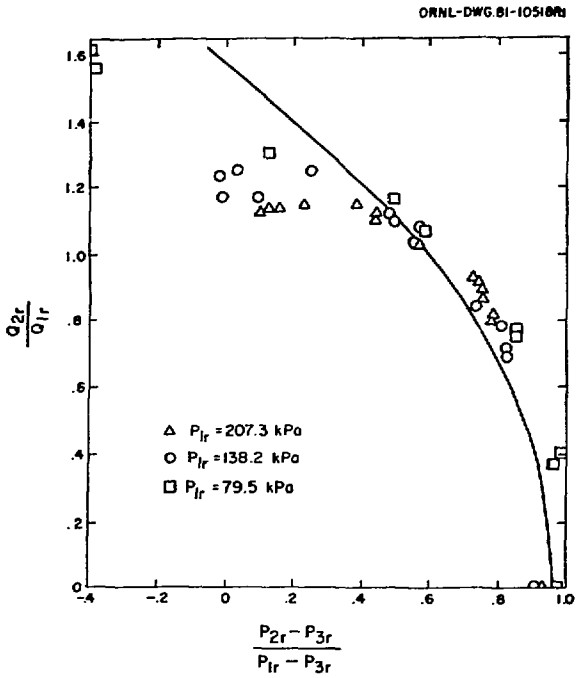

Fig. 10. Normalized output characteristics of the reverse flow diverter.

6 Acknowledgements

This work was performed in the Fuel Recycle Division under the auspices of the Consolidated Fuel Reprocessing Program of the Oak Ridge National Laboratory and was sponsored by the Office of Nuclear Fuel Cycle, U.S. Department of Energy, under Contract No. W-7405-eng-26 with Union Carbide Corporation.

Nomenclature

A	area
C_d	discharge coefficient
C_p	pressure recovery coefficient
K_d	diffuser loss coefficient
P	pressure
Q	volumetric flow rate
V	velocity
ρ	density
h_o	output hydrostatic head

Subscripts

f	forward flow mode
r	reverse flow mode
s	source
t	throat
1	port 1 of RFD
2	port 2 of RFD
3	port 3 of RFD

References

1. J. H. Mammon, "Fluidics Score in Quest for CPI Applications," *Chem. Eng.* 87, 33–7 (July 1980).

2. J. C. Campbell and R. F. Jackson, "Review of Remote Handling Experience and Philosophy in a Reprocessing Plant in the United Kingdom," pp. 186–205 in *Proc. 25th Conf. Remote Systems Technology*, American Nuclear Society, San Francisco (1977).

3. J. P. Baker, "A Comparison of Fluidic Diodes," *Second Cranfield Fluidics Conf.*, Cambridge, England, D6-(88-115) (January 1967).

4. B. E. A. Jacobs, "Fluidic Diodes," in *Proc. of the Symposium for Process Control*, pp. 11–9, University of Surrey, Gilford, England (1973).

5. J. R. Tippetts, "A Fluidic Pump for Use in Nuclear Fuel Reprocessing," *Proc. of the 5th International Fluid Power Symposium*, University of Durham, England (1978).

6. J. R. Tippetts, "Some Recent Developments in Fluidic Pumping," *Proc. of Pumps 1979, 6th Technical Conf. of the British Manufacturers Association*, Canterbury, England (1979).

7. J. M. Kirshner, *Jet Dynamics and Its Applications to the Beam Deflection Amplifier*, HDL-TR-1630, Harry Diamond Laboratories, Washington, D.C. (July 1973).

8. P. W. Runstadler, Jr., F. X. Dolan, and R. C. Dean, Jr., *Diffuser Data Book*, TN-186, Creare Technical Information Service, Hanover, N.H. (1975).

9. R. W. Fox and S. J. Kline, *J. Basic Eng.* 84, 303–12 (1962).

10. K. N. Reid, *Static and Dynamic Interaction of a Fluid Jet and a Receiver-Diffuser*, Sc.D. thesis, Department of Mechanical Engineering, Massachusetts Institute of Technology, Cambridge, Mass. (1964).